TDA Progress Report 42-99

November 15, 1989

Microwave Oscillator With Reduced Phase Noise by Negative Feedback Incorporating Microwave Signals With Suppressed Carrier

G. J. Dick and J. Saunders
Communications Systems Research Section

This article develops and analyzes oscillator configurations which reduce the effect of $1/f$ noise sources for both direct feedback and stabilized local oscillator (STALO) circuits. By appropriate use of carrier suppression, a small signal is generated which suffers no loss of loop phase information or signal-to-noise ratio. This small signal can be amplified without degradation by multiplicative amplifier noise, and can be detected without saturation of the detector. Together with recent advances in microwave resonator Qs, these circuit improvements will make possible lower phase noise than can be presently achieved without the use of cryogenic devices.

I. Introduction

Phase fluctuations in microwave oscillators show a characteristic $1/f^3$ spectral density for frequencies very close to the carrier. The spectral density $S_\phi(f)$ can be expressed in terms of rad^2 per Hz bandwidth at an offset frequency f from the carrier. At larger frequency offsets ($f > 10$ kHz), fluctuations decrease more slowly, typically approaching a more or less constant value for frequencies of 100 kHz and above. This article is concerned with reduction of the fluctuations very close to the carrier by the use of circuit techniques not previously applied to microwave oscillators.

In order to achieve a microwave signal with the lowest possible noise at all offset frequencies, a variety of technologies is presently used [1, 2, 3]. Typically, high stability for small offsets ($f < 100$ Hz) is obtained by locking the microwave oscillator to a harmonic of a low-frequency (5 MHz) bulk acoustic wave (BAW) quartz-crystal oscillator. For offset frequencies in the range of 100 Hz $< f <$ 10 kHz, further stabilization may be provided by a surface acoustic wave (SAW) oscillator operating at $\approx$ 500 MHz. The microwave oscillator itself provides the best possible stability only for relatively large offset frequencies ($f \geq$ 10 kHz).

While all the sources listed above show $1/f^3$ type phase fluctuations for small values of offset frequency f, the microwave oscillator itself shows by far the highest noise. This is due to two contributing factors: the low Q available for microwave resonators and the large $1/f$

phase noise in available microwave devices. (The action of the oscillation loop converts this $1/f$ phase noise into $1/f$ frequency noise, which is mathematically equivalent to $1/f^3$ phase noise [1, 16].) Thus, while BAW and SAW quartz crystals show Qs of 10^6 and 10^5 respectively, microwave cavities and dielectric resonators are limited to Qs in the range 1–3 $\times 10^4$. In like manner, active devices which are available at the lower operating frequencies of the quartz devices show $1/f$ phase noise of -140 dB per Hz or lower at an offset frequency of $f = 1$ Hz, while the best 8–12 GHz (X-band) amplifiers have noise of -120 dB per Hz [13, 14].

Recently, a new type of microwave resonator has been demonstrated with Qs 10 to 1000 times larger than previously available [4–11]. This sapphire whispering-gallery-mode resonator allows the intrinsic Q of the sapphire itself to be utilized by isolating the fields to the sapphire element and away from lossy metallic container walls. These resonators have shown Qs of 2×10^5 at room temperature and 3×10^7 at 77 K. Tests of an 8-GHz oscillator stabilized by such a sapphire resonator (a stabilized local oscillator, or STALO) show $1/f^3$ noise 10 dB lower than previously reported for any 8–12 GHz (X-band) source and only 22 dB higher than the best quartz-crystal stabilized oscillator [9, 12]. If the device noise in this oscillator could be reduced by 20 dB or more, the need for quartz stabilization would be eliminated, and a new oscillator capability would become available.

The following sections describe two substantially different implementations of an idea in which negative feedback in the oscillator is generated by means of a suppressed-carrier microwave signal. In one implementation, the signal is fed to a semiconducting phase detector to enhance its sensitivity while avoiding saturation. In this STALO configuration, phase-detector noise is effectively reduced by the enhanced sensitivity. In the second implementation, direct RF feedback of a signal with suppressed carrier induces both oscillation and negative phase feedback. In this case, the degree of improvement in $1/f$ phase noise over that which characterizes the amplifier itself is equal to the degree of negative feedback which can be achieved without oscillation in unwanted modes.

A comparison of the two implementations shows the second (direct RF feedback) to be somewhat trickier in concept (involving both negative-phase feedback and positive-amplitude feedback in the same loop), and simpler in realization. Conditions of stability require the use of a filter with a performance that is expected to limit the usable loop gain to the 20–30 dB range. The STALO-type implementation, while more elaborate, is somewhat less tricky, and should allow larger gains to be used. Both should show crystal-oscillator-type performance in a room-temperature 10-GHz (X-band) oscillator using a whispering-gallery-mode sapphire resonator with an intrinsic Q of 2×10^5, and allow dramatic improvements in the state of the art with cooled resonators and higher Qs.

II. Background

Figures 1 and 2 show conventional microwave self-excited oscillator and STALO configurations, together with an identification of the in-oscillator and oscillator output noise spectral densities. In the self-excited oscillator shown in Fig. 1, the oscillation condition requires that the phase shift around the complete feedback loop comprising the amplifier, resonator, and interconnections be a multiple of 2π. With this condition satisfied, any phase fluctuation in the microwave amplifier must be accompanied by an opposite shift of equal magnitude in the resonator. For slow phase fluctuations ($f \ll \nu/Q$), the characteristic phase slope of the resonator $\delta\phi/\delta\nu = 2Q/\nu$ implies a corresponding slow fluctuation in the frequency of the oscillator. Here f represents the fluctuation frequency, ν the microwave frequency, Q the quality factor of the resonator, and ϕ the phase of the microwave signal. In this way, a power spectral density of phase fluctuations for the amplifier $S_\phi(f)\,|_{amp}$ results in oscillator output frequency noise

$$S_y(f)\,|_{out} = (2Q)^{-2} S_\phi(f)\,|_{amp}$$

or the mathematically equivalent output phase fluctuations

$$S_\phi(f)\,|_{out} = (2Q)^{-2} \left(\frac{\nu}{f}\right)^2 S_\phi(f)\,|_{amp} \qquad (1)$$

where $y \equiv \delta\nu/\nu$ is the fractional frequency deviation.

Figure 2 shows the schematic diagram for a STALO in which the frequency variations of a noisy microwave source are cancelled by a feedback loop that detects the consequent phase shifts across a high-Q resonator to generate a frequency-correction voltage. The phase from the reference loop is adjusted to produce the proper sign of the correction voltage and attain maximum sensitivity by operating in the high slope region of the mixer output versus reference phase relation. In the limit of large loop gain, stable equilibrium requires that the phases at the two input ports of the mixer be in quadrature (mixer output = zero). A significant advantage of the STALO is that the properties of the feedback loop are particularly easy to control, since the signal is mixed down to baseband (near zero frequency). This allows the use of active filters with narrow

bandwidths and sophisticated response shapes which are not possible at microwave frequencies. A second advantage is that the $1/f$ noise for X-band mixers (-135 dB/f per Hz at 10 GHz) [15] is better than that which is available from the best amplifiers (-110 to -120 dB/f) [13, 14]. The analysis from the self-excited oscillator can be adapted to the STALO by noting that the only difference is that the phase detection and correction has been moved from the resonator in Fig. 1 to the mixer-amplifier-oscillator combination in Fig. 2. The phase noise of the RF amplifier of Fig. 1 is replaced by that of a mixer. Consequently, the output phase fluctuations are described by

$$S_\phi(f)\,|_{out} = (2Q)^{-2}\left(\frac{\nu}{f}\right)^2 S_\phi(f)\,|_{mix}$$

As a consequence, the performance of a direct-feedback oscillator with an amplifier having $1/f$ noise of -120 dB per Hz at 1 Hz ($S_\phi(f)\,|_{amp} = 10^{-12}/f$ rad^2 per Hz) is

$$S_\phi(f)\,|_{out} = 10^{-12}(2Q)^{-2}\left(\frac{\nu^2}{f^3}\right)$$

while a STALO using a mixer with $S_\phi(f)\,|_{mix} = 10^{-13.5}/f$ rad^2 per Hz will be 15 dB quieter. These device noise levels represent the quietest components presently available, giving a clear advantage to the STALO configuration.

III. Oscillator Configurations for Reduced Noise

Three new oscillator configurations for low phase noise are detailed in this section. The first two are STALO configurations that reduce the effect of mixer noise by increasing its sensitivity by the use of a suppressed-carrier signal. Of these two, the first achieves increased sensitivity by operating the high-Q resonator at higher power than would otherwise be possible. In the second, a similar effect is achieved by use of a low-level RF amplifier. The third oscillator configuration uses direct RF feedback of a sort that simultaneously achieves positive-amplitude feedback and negative-phase feedback. In this way excess gain of the amplifier is used to reduce its effective phase noise.

The STALO shown in Fig. 3 forms the basis for the new designs. It differs in implementation from Fig. 2 in that the signal from the cavity to the mixer is not taken from a second coupling port but is instead taken from the signal reflected from the input port. A circulator separates this signal from the forward-driving signal. At critical coupling and on resonance, the returned signal is identically zero. However, it is the superposition of two equal signals, one of which emanates from the cavity, and a second, reflected signal which is derived from the driving signal with a constant phase shift. This reflected signal does not significantly affect the operation of the mixer at resonance since it is in quadrature with the signal at the other mixer port. Thus the two STALOs will have approximately identical performance. Figure 4 shows the returned signal for small errors in local oscillator frequency. While the amplitude goes through zero on resonance, a phase reversal takes place in which the in-phase signal on one side becomes out of phase on the other, allowing a linear dependence of mixer output voltage on the frequency error, as required for effective feedback. Instead of viewing the mixer as a phase detector, it is seen as projecting the component of the signal at the r input onto the phase of that at the l input.

A. STALO Design for Enhanced Phase Detector Sensitivity

In this configuration, enhanced sensitivity in the phase detector is achieved by means of relatively high power in the high-Q resonator. It has the advantages of simplicity and absence of any amplifier to introduce added phase noise if carrier suppression is incomplete. A disadvantage is that power limitations in the microwave source or high-Q resonator restrict the available improvement factor.

As previously discussed and as shown in Fig. 5(a), suppression of the carrier at the r port of the mixer in Fig. 3 has only incidental consequence regarding mixer sensitivity, since the suppressed part of the signal is in quadrature with the reference signal at the l port. (The part of the signal due to frequency variations, $\pm\delta\nu$, is in phase with the reference and so is detected in any case.) However, things are not quite identical to the conventional STALO shown in Fig. 2. Suppression of the carrier at the r port allows the power to the high-Q resonator to be increased without saturating the mixer. This increased power results in an enhanced sensitivity of the mixer output voltage to frequency variations $\pm\delta\nu$.

Figure 6 describes such a circumstance. Besides the increased power levels in oscillator and resonator, the only difference from Fig. 3 is an appropriately weaker coupling to the mixer's l port. Mixers typically saturate at signal levels on the order of 20 milliwatts, while frequency sources and resonators can operate at power levels up to 1 watt or even higher. The resultant increase in sensitivity of up to 17 dB reduces the consequence of mixer noise by the same factor. For a mixer with flicker noise of -135 dB per Hz at 1 Hz offset, the effective noise could be reduced to a value of -152 dB per Hz.

B. STALO Design Using RF Amplification

Figure 7 shows a further modification of the STALO which can result in improved performance. Here the small, nominally zero signal returned from the resonator is amplified before it enters the mixer. Two effects of this addition are easy to understand. The loop gain will be increased by the added gain, an effect which may be compensated for in the design of the baseband amplifier. Secondly, the gain of the amplifier will increase the sensitivity of the mixer output to phase error in the resonator without significantly affecting mixer noise. Thus the effective mixer phase noise is reduced by the amount of amplifier gain. This can be a very substantial improvement.

The third effect of this modification is a little more complicated. Since amplifiers are somewhat more noisy than mixers (−120 dB versus −135 dB at 1 Hz offset as previously discussed), a crucial point is the proper analysis of the contribution of amplifier noise. The kind of noise under discussion is not additive noise, which would be independent of any large signal also present, but instead is multiplicative noise, which transforms a large signal by slightly modifying its amplitude and phase. (Additive noise in good amplifiers is insignificant except at offset frequencies $f > \approx 10$ kHz where the $1/f$ multiplicative noise is relatively small.) Figure 5(a) shows in phasor form the cavity signals with and without carrier suppression corresponding to the oscillators shown in Figs. 3 and 2, respectively. The added signals due to small frequency variation in the local oscillator are also shown. These added signals are detected by the mixer in order to allow feedback circuitry to cancel the frequency variations. The effect of multiplicative phase noise in the amplifier for the two cases is shown in Fig. 5(b). It is clear from Fig. 5(b) that this noise source generates signals which are indistinguishable from those caused by actual frequency variations, and which are due only to the presence of the coherent carrier. Thus a reduction in amplifier noise is effected which is proportional to the degree of carrier suppression of the microwave signal at its input.

Oscillator phase noise is thus determined by a combination of mixer noise (reduced by amplifier gain) and amplifier noise (reduced by the degree of carrier suppression). For example, if mixer noise of -135 dB/f per Hz were reduced by 25 dB of amplifier gain to -160 dB/f per Hz, and amplifier noise of -120 dB/f per Hz were reduced by 40 dB of carrier suppression to the same value, the combined noise of -157 dB/f per Hz would determine oscillator performance. For a loaded Q of 10,000 (intrinsic $Q = 20,000$), this would allow an oscillator phase noise of $S_\phi(f)|_{osc} = -43$ dB/f^3 per Hz, a value superior to any room-temperature microwave oscillator to date. For room temperature and thermoelectrically cooled sapphire resonators with Qs of 10^5 and 10^6, performance would be superior to that of any available source at $S_\phi(f)|_{osc} = -63$ dB/f^3 per Hz and -83 dB/f^3 per Hz, respectively.

C. Oscillator With RF Feedback

1. Noise reduction. Figure 1 shows a conventional microwave oscillator excited by direct RF feedback. As discussed earlier, any slow phase shift in the amplifier is converted by the feedback process into a frequency shift of the oscillator output as required by the condition of constant phase shift around the loop ($\phi_{loop} = 2n\pi$), with the conversion constant depending on the resonator Q. The total signal returned from the input port to the resonator is the superposition of two parts, a reflected constant signal equal in magnitude to the input signal, and an emitted part proportional to the instantaneous RF amplitude in the resonator. In the previous section, the critically coupled case was discussed, where on resonance the net returned signal was identically zero. If instead the cavity is slightly over-coupled, so that the signal emitted from the resonator is larger than the reflected signal, the net signal returned from the resonator will not be zero on resonance but will have a small, constant value. Figure 8(a) shows the configuration for an oscillator in which the small returned signal is amplified and returned to the cavity to induce oscillation. RF feedback of a phase and magnitude that allows oscillation on resonance will also induce negative phase feedback that reduces the effect of amplifier phase fluctuations on the oscillator frequency.

Figure 9(a) shows these various signals in phasor form for the case $Q \gg 1$, with weak magnetic coupling to the resonator achieved by means of an iris at the end of a waveguide or by a shorted coaxial line. Shown are the forward signal voltage amplitude $\vec{f}$, reflected signal $\vec{r}$ (directly reflected by the coupling port), emitted signal $\vec{e}$, and net returned signal $\vec{n}$, as shown for the condition of resonance (test frequency = resonator frequency.) Signals are measured at the effective plane of the weak coupling port. For frequencies significantly outside the bandwidth of the resonator, the net returned signal is approximately equal to $\vec{r}$; thus, out-of-bandwidth oscillation is prevented by the phase reversal between $\vec{n}$ and $\vec{r}$. In order to achieve oscillation at resonance, the gain and phase shift around the loop must regenerate $\vec{f}$ from $\vec{n}$. For the slightly over-coupled case shown, this corresponds to a net phase shift $2\vec{n}\pi$, and gain to overcome the signal amplitude reduction $|\vec{f}/\vec{r}|$. While small losses due to transmission through various circuit elements must also be made up by the gain element, they can be ignored for this analysis.

Intrinsic and external Qs, Q_i and Q_e, describe the effect of resonator and coupling losses and combine to form the loaded Q_l

$$Q_l^{-1} = Q_i^{-1} + Q_e^{-1}$$

which defines the operational bandwidth of the resonator. Using standard circuit analysis, the amplitude of the resonator response to the forward signal can be written:

$$\frac{|\vec{e}|}{|\vec{f}|} = \frac{2q}{q+1} \times \frac{1}{\sqrt{1+\left(2Q_l\delta\nu/\nu_o{}^2\right)}} \tag{2}$$

where $q \equiv Q_i/Q_e$ is a loading factor, ν_o is the resonance frequency, and $\delta\nu$ is the frequency deviation from resonance. The phase of the resonator response is similarly given by

$$\tan(\phi) = \frac{2Q_l\delta\nu}{\nu_o} \tag{3}$$

for a slope at resonance of

$$\frac{\delta\phi}{\delta\nu} = \frac{2Q_l}{\nu_o} \tag{4}$$

Now calculate the amplifier gain required for oscillation at resonance ($\delta\nu \approx 0$). From the nature of the coupling,

$$\vec{r} = -\vec{f} \tag{5}$$

and from the equation above

$$\vec{e} = \vec{f} \times \frac{2q}{q+1}$$

These can be combined to give

$$\vec{n} = \vec{r} + \vec{e} = \vec{f} \times \frac{q-1}{q+1}$$

requiring a gain of

$$G = \frac{|\vec{f}|}{|\vec{n}|} = \frac{q+1}{q-1} \tag{6}$$

for oscillation. The over-coupled condition depicted in Fig. 9 corresponds to $q > 1$. If $q \equiv 1 + \delta q$, the gain requirement can be rewritten as

$$G = \frac{2}{\delta q} + 1 \tag{7}$$

For the oscillator shown in Fig. 1, a small phase shift θ in the amplifier gives a corresponding phase shift $-\theta$ across the resonator, with a resultant frequency shift given by the phase slope in Eq. (4). The configuration shown in Fig. 8(a) gives a reduced resonator phase shift and thus reduced frequency shift. This reduction is now calculated. Figure 9(b) shows the self-consistent phasor diagram for the oscillator of Fig. 8(a), with a slight amplifier phase shift θ. The instantaneous frequency is determined by the smaller angle ϕ, together with the resonator phase slope $2Q_l/\nu_o$; thus, the ratio ϕ/θ describes the phase noise reduction of Fig. 7 compared to Fig. 1. The diagram is oriented so that the direction of e is constant. Graphically solving $\vec{n} = \vec{e} + \vec{r}$ shows that the effect of a rotation θ between $\vec{n}$ and $\vec{f}$ due to the amplifier gives an angle ϕ between $\vec{f}$ and $\vec{e}$. The angle ϕ in turn determines the frequency shift via Eq. (3). A straightforward evaluation for the geometry shown gives

$$\theta = \phi + \sin^{-1}\left(\frac{|\vec{r}|}{|\vec{n}|} \times \sin(\phi)\right)$$

which can be approximated in the limit of small angles to give

$$\phi/\theta \approx \frac{1}{1 + \frac{|\vec{r}|}{|\vec{n}|}} \tag{8}$$

This approximation will hold to high degree of accuracy because of the very small value of the phase fluctuations involved. Using Eqs. (6) and (5), Eq. (8) can be rewritten in terms of the amplifier gain as

$$\phi/\theta \approx \frac{1}{1+G}$$

The factor ϕ/θ describes the reduction in phase variation across the cavity compared to that across the amplifier. It also describes the improvement in performance due to the circuit in Fig. 8(a). Combining this result with Eq. (1), the phase-noise performance of the oscillator is

$$S_\phi(f)\,|_{out} = (\phi/\theta)^2(2Q_l)^{-2}\left(\frac{\nu}{f}\right)^2 S_\phi(f)\,|_{amp}$$

For example, for $G = 10$ (20 dB of amplification), ϕ/θ is 1/11 (22 dB of noise reduction). If the amplifier has noise

of -120 dB/f per Hz (or $S_\phi(f)\,|_{amp} = 10^{-12}/f$ rad^2 per Hz), oscillator performance will be

$$S_\phi(f)\,|_{out} = 0.8 \times 10^{-14}(2Q_l)^{-2}\left(\frac{\nu^2}{f^3}\right)$$

which for a frequency of 10 GHz and Q_l of 10^5 gives

$$S_\phi(f)\,|_{out} = 2 \times 10^{-5}/f^3$$

or -47 dB per Hz at $f = 1$ Hz offset frequency. For this same case, Eq. (7) shows that the degree of over-coupling required is

$$\delta q = \frac{2}{G-1} = \frac{2}{9}$$

or

$$\frac{Q_i}{Q_e} = 1 + \delta q = \frac{11}{9}$$

and

$$Q_l = \frac{1}{Q_e^{-1} + Q_i^{-1}} = Q_i \times \frac{1}{11/9+1} = 0.45 \times Q_i$$

2. Loop stability. The oscillation condition for the direct RF feedback configuration is such that the directly reflected signal has a net phase shift of 180 deg with respect to the signal emitted from the resonator. Thus the loop will not oscillate at frequencies outside the passband of the stabilizing resonator (where very little signal is absorbed or emitted by the resonator), unless the phase is shifted by other elements in the circuit. Unfortunately, the path length of the circuit alone is sufficient to add such a shift if the frequency is slightly varied. Thus, for a path length of 10λ, a 180-deg phase shift will occur with a 5-percent frequency change. Even worse, at these ± 5-percent frequencies, the loop gain will be nearly G, a value much greater than the loop gain at the desired mode (approximately unity). These oscillations do not involve any high-Q resonance, and can only be prevented by the introduction of a filter whose function is to reduce the gain (as the frequency is varied away from ν_o) to a value less than unity by the time the phase shift due to all sources reaches 180 deg. Because each stage of a filter introduces a phase shift of ≈ 90 deg by the time substantial attenuation is achieved, a single-stage filter must be used. The phase margin for the rest of the circuit is thus reduced to ≈ 90 deg by the filter's presence. Because a single-stage filter attenuates relatively slowly as the frequency is varied, a narrow bandwidth is required. For the example here, with a path length of 10λ and for $G = 10$ (20 dB), filter attenuation of 20 dB must be achieved at a frequency offset of 2.5 percent, where the circuit length alone introduces a 90-deg shift. This requires a filter bandwidth of ≈ 0.25 percent, a value that can be achieved with low loss using conventional techniques.

The expressions for amplitude response and phase shift for a single-stage filter are identical to those already presented in Eqs. (2) and (3). The shift due to a transmission line is given by

$$\delta\phi = 2\pi\left(\frac{p}{\lambda}\right)\left(\frac{\delta\nu}{\nu_o}\right)$$

where p is the effective path length. Figure 8(b) shows an oscillator with the added filter; Figs. 10 and 11 show the amplitude and phase response for a single-stage filter with $Q = 3000$, and the added phase due to an effective path length of 1 m. For Fig. 11, an attenuation of 35 dB is generated before the total phase shift reaches 180 deg, thus allowing $\leq 35\ dB$ of loop gain for the reduction of amplifier phase noise. It can be seen from the figures that the attenuation of this filter is nearly 35 dB by the time the total phase variation due to filter and transmission path reaches 180 deg. While 3000 is a relatively high Q for a single-mode filter, it can be attained with low loss. It is clear that usable gain and consequent usable noise reduction of 20 to 30 dB can be achieved with this technique.

IV. Conclusions

Typical low-noise 10-GHz (X-band) oscillators use a single transistor or other active semiconducting device for excitation; while a more elaborate STALO configuration is used for the lowest possible phase noise. With the development of sapphire whispering-gallery-mode resonators with Qs above 10^5 to 10^7 at 10 GHz, the possibilities have been considerably enhanced. Whereas lower frequency SAW or BAW quartz-crystal oscillators had far lower noise than their higher frequency counterparts, they are rivalled by an X-band oscillator using the sapphire resonator [9]. Together with the improved oscillator circuits developed here, such a resonator may make possible close-in phase noise lower than that of any noncryogenic frequency source. Furthermore, cooling by means of thermoelectric coolers or liquid nitrogen may make practical frequency sources with greatly reduced phase noise.

New design configurations for STALOs and direct RF oscillators allow reduced phase noise in comparison to conventional configurations. By appropriate use of carrier sup-

pression, a small signal is generated which suffers no loss of loop-phase information or signal-to-noise ratio. This small signal can be amplified without degradation by multiplicative amplifier noise, and can be detected without saturation of the detector.

Figure 12 shows phase-noise calculations for an improved sapphire whispering-gallery-mode oscillator and STALO for configurations as shown in Figs. 8 and 7. Use of a cryogenic sapphire resonator allows a further improvement of 20 to 43 dB. Quality factors are assumed to be $Q_i = 2 \times 10^5$ at room temperature, $Q_i = 2 \times 10^6$ at 170 K, and $Q_i = 3 \times 10^7$ at 77 K. Noise plots for various conventional 10-GHz frequency sources are also shown. The multiplied 5-MHz crystal oscillator presently represents the best performance available at X-band.

References

[1] W. P. Robins, *Phase Noise in Signal Sources*, IEE Telecommunications Series 9, London: Peter Peregrinus Ltd., 1984.

[2] G. K. Montress, T. E. Parker, M. J. Loboda, and J. A. Greer, "Extremely Low Phase Noise SAW Resonators and Oscillator: Design and Performance," *IEEE Trans. Ultrasonics, Ferroelectrics, and Frequency Control*, vol. UFFC-35, no. 6, pp. 657–667, 1988.

[3] R. G. Rogers, "Theory and Design of Low Phase Noise Microwave Oscillators," *Proc. 42nd Ann. Symposium on Frequency Control*, pp. 301–303, 1988.

[4] D. G. Blair and S. K. Jones, "High-Q Sapphire Loaded Superconducting Cavities and Application to Ultrastable Clocks," *IEEE Trans. Magnetics*, vol. MAG-21, pp. 142–145, March 1985.

[5] A. Giles, S. Jones, and D. Blair, "A High Stability Microwave Oscillator Based on a Sapphire Loaded Superconducting Cavity," *Proc. 43rd Ann. Symposium on Frequency Control*, pp. 89–93, 1989.

[6] V. B. Braginsky, V. P. Mitrofanov, and V. I. Panov, *Systems With Small Dissipation*, Chicago: University of Chicago Press, pp. 85–89, 1985.

[7] V. I. Panov and P. R. Stankov, "Frequency Stabilization of Oscillators With High-Q Leucosapphire Dielectric Resonators," *Radiotekhnika i Electronika*, vol. 31, no. 213, 1986 (in Russian).

[8] G. J. Dick and D. M. Strayer, "Measurements and Analysis of Cryogenic Sapphire Dielectric Resonators and DRO's," *Proc. 41st Ann. Symposium on Frequency Control*, pp. 487–491, 1987.

[9] J. Dick and J. Saunders, "Measurement and Analysis of a Microwave Oscillator Stabilized by a Sapphire Dielectric Ring Resonator for Ultra-Low Noise," *Proc. 43rd Ann. Symposium on Frequency Control*, pp. 107–114, 1989.

[10] X. H. Jiao, P. Guillon, and L. A. Bermudez, "Resonant Frequencies of Whispering-Gallery Dielectric Resonator Modes," *IEE Proceedings*, vol. 134, pt. H, pp. 497–501, 1987.

[11] M. Gastine, L. Courtois, and J. L. Dormann, "Electromagnetic Resonances of Free Dielectric Spheres," *IEEE Trans. Microwave Theory and Techniques*, vol. MTT-15, pp. 694–700, December 1967.

[12] M. M. Driscoll, "Low Noise Signal Generation Using Bulk- and Surface-Acoustic-Wave Resonators," *IEEE Trans. Ultrasonics, Ferroelectrics, and Frequency Control*, vol. UFFC-35, no. 3, pp. 426–434, 1988.

[13] T. E. Parker, "Characteristics and Sources of Phase Noise in Stable Oscillators," *Proc. 41st Ann. Symposium on Frequency Control*, pp. 99–110, 1987.

[14] C. P. Lusher and W. N. Hardy, "Effects of Gain Compression, Bias Conditions, and Temperature on the Flicker Phase Noise of an 8.5 GHz GaAs MESFET Amplifier," *IEEE Trans. on Microwave Theory and Techniques*, vol. 37, pp. 643-646, April 1989.

[15] F. L. Walls, A. J. D. Clements, C. M. Felton, M. A. Lombardi, and M. D. Vanek, "Extending the Range and Accuracy of Phase Noise Measurements," *Proc. 42nd Ann. Symposium on Frequency Control*, pp. 432–441, 1988.

[16] J. A. Barnes, R. Chi, L. S. Cutler, D. J. Healey, D. B. Leeson, T. A. McGunigal, J. A. Mullen, Jr., W. L. Smith, R. L. Sydnor, R. F. C. Vessot, and G. M. R. Winkler, "Characterization of Frequency Stability," *IEEE Trans. Instr. and Meas.*, vol. IM-20, pp. 105–120, May 1971.

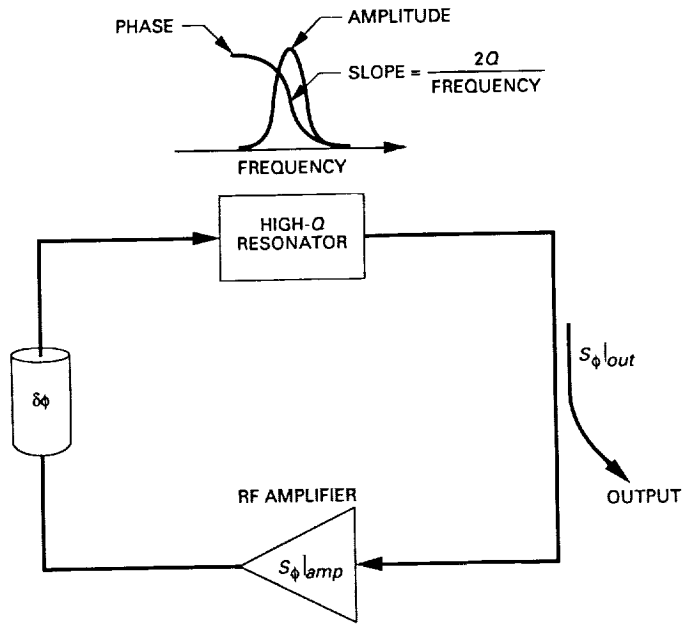

Fig. 1. Block diagram of simple oscillator with direct RF feedback. Output phase noise is derived from amplifier noise together with phase slope of resonator; phase is adjusted to give 2 $n\pi$ radians around loop at the center of the sapphire resonator passband.

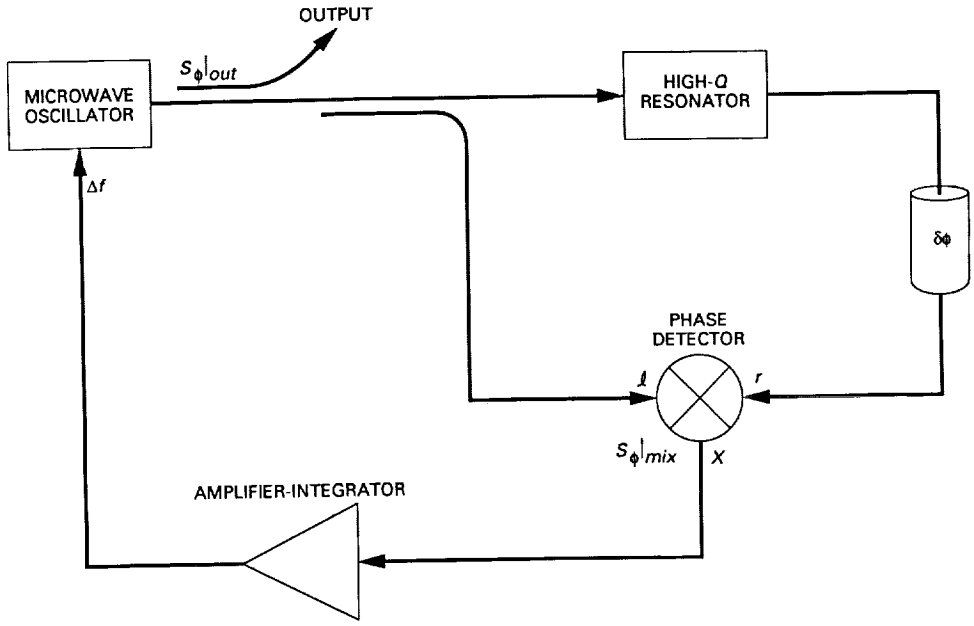

Fig. 2. Block diagram of stabilized local oscillator (STALO) with double-balanced mixer type phase detector. Mixer noise plays the same role as amplifier noise in Fig. 1; phase is adjusted to give *l* and *r* signals in quadrature.

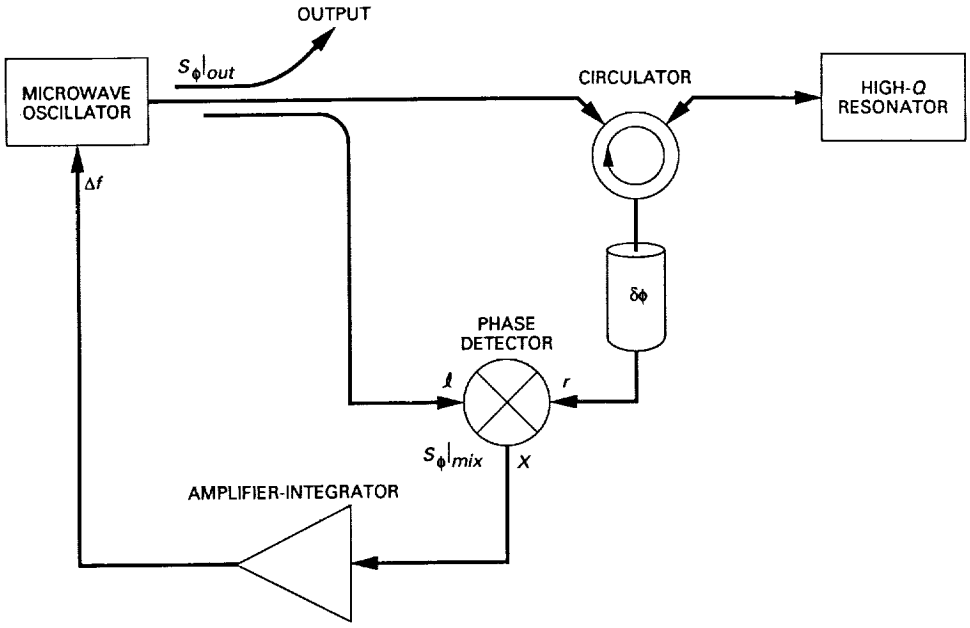

Fig. 3. STALO with different configuration but functionally identical to that of Fig. 2. Signal returned from resonator is superposition of the resonator signal and the constant reflected signal.

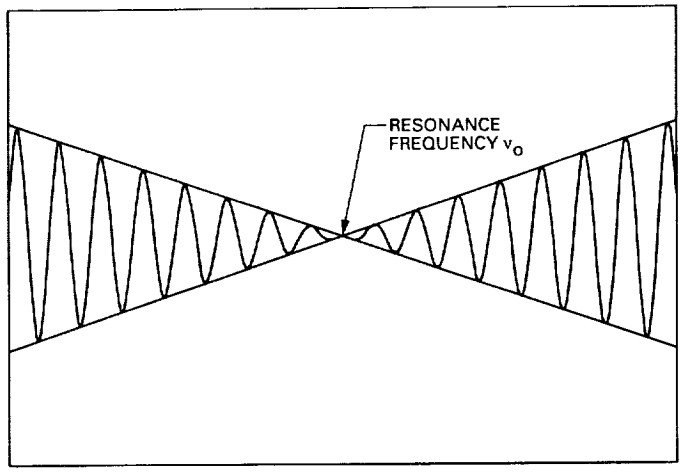

Fig. 4. RF envelope of returned signal for critical coupling as frequency ν is varied. Phase inversion at center allows linear dependence in mixer output with frequency for arbitrarily small frequency errors.

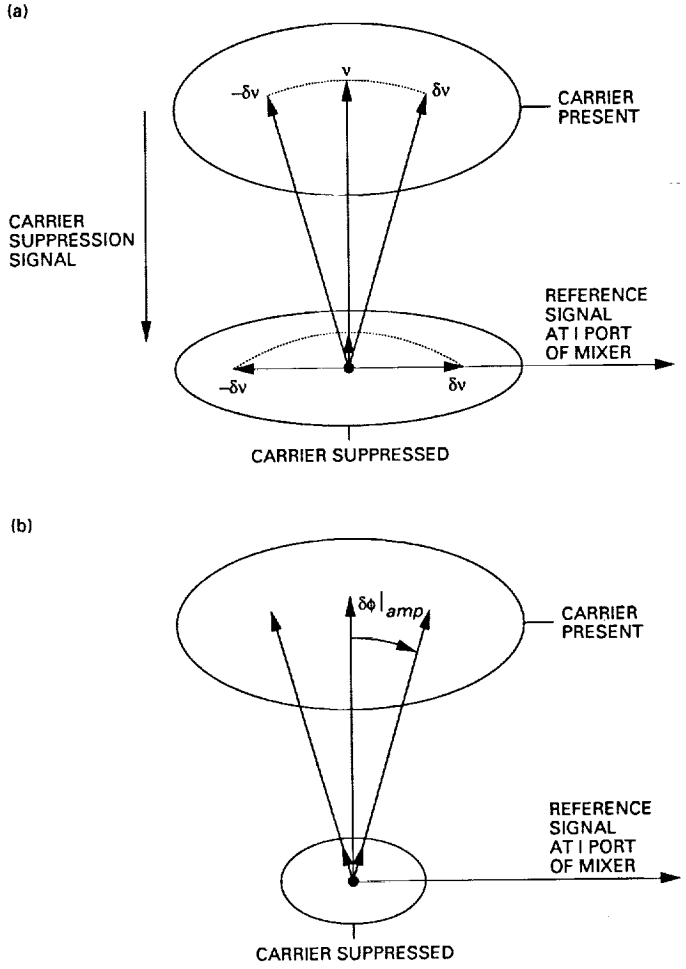

Fig. 5. Phasor diagram showing the effect, with and without carrier suppression, of (a) frequency error and (b) amplifier phase noise on the RF resonator signal. Also shown are the constant carrier suppression signal and mixer reference signal. Note that the effect of frequency error on the component of the RF resonator signal in phase with the reference is unchanged by 20 dB carrier suppression, while the effect of amplifier phase noise is reduced by 20 dB.

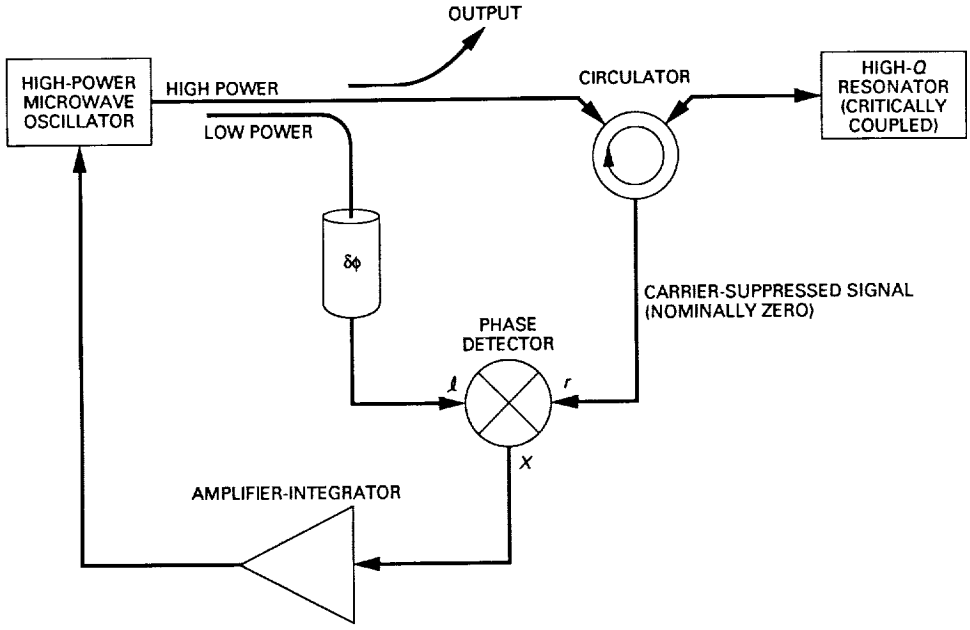

Fig. 6. Configuration to allow increased power into the high-Q resonator without saturating the mixer; the resultant increase in sensitivity of up to 17 dB reduces the consequence of mixer noise by the same factor.

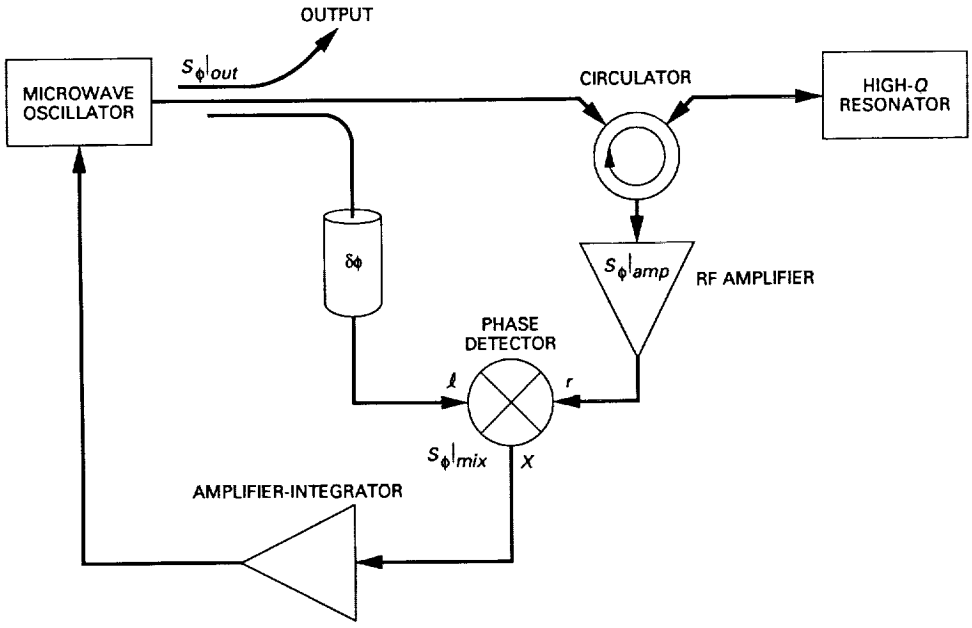

Fig. 7. STALO configuration for reduced phase noise. Critical coupling to resonator and operation very near ν_o allow insensitivity to phase noise of amplifier; amplifier gain allows reduction of phase detector noise.

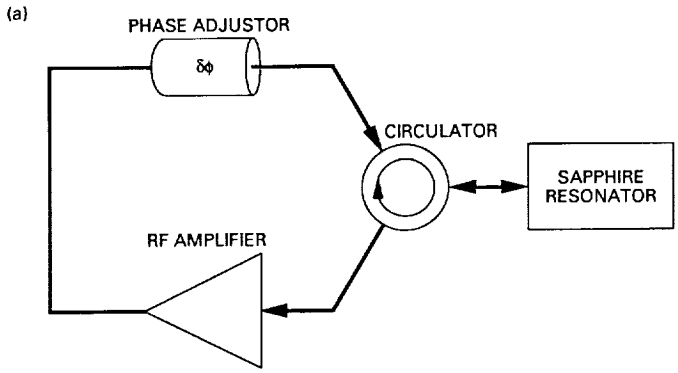

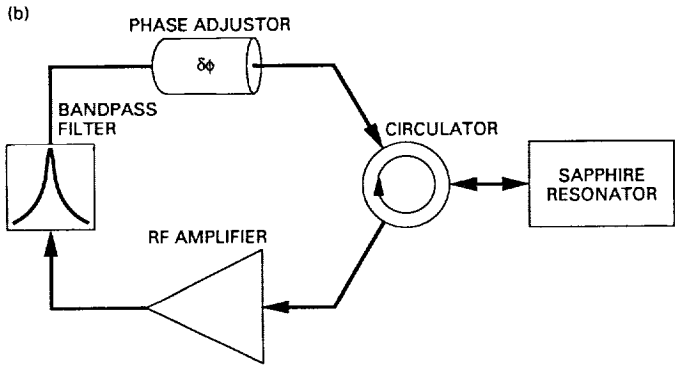

Fig. 8. Configuration of reflection oscillator: (a) with direct RF feedback, (b) added filter prevents spurious oscillation.

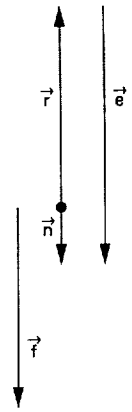

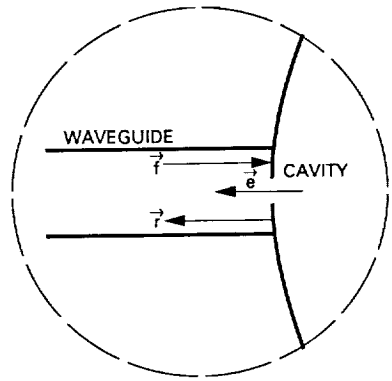

Fig. 9(a). Phasor diagram showing forward, reflected, emitted, and net signal amplitudes $\vec{f}$, $\vec{r}$, $\vec{e}$, and $\vec{n}$, for a slightly over-coupled resonator at resonance.

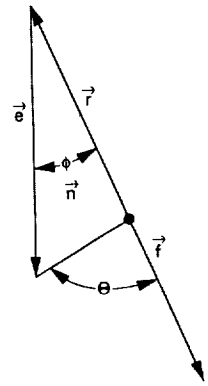

Fig. 9(b). Self-consistent phasor diagram showing the effect of amplifier phase shift θ on operation of the oscillator shown in Fig. 7. Feedback gain is the same as in Fig. 9(a).

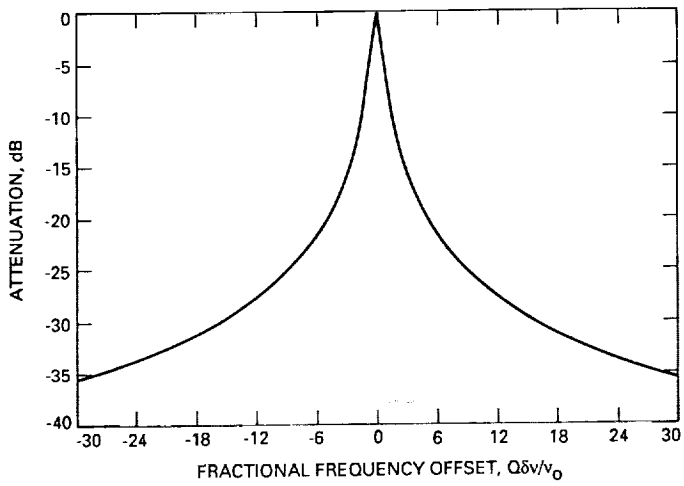

Fig. 10. Amplitude response of the single-stage filter in Fig. 8(b). More stages cannot be used because the added phase shift would allow oscillation within the filter bandwidth.

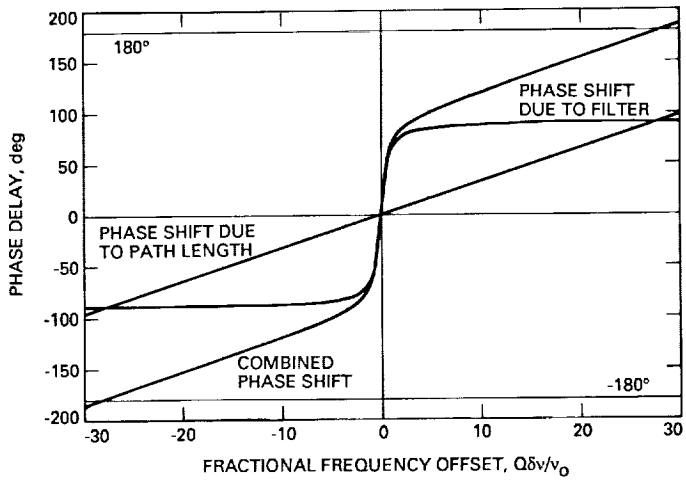

Fig. 11. Phase response of the single-stage filter together with phase response due to path lengths, for path length of 1 m, Q = 3000, and ν_0 = 8 GHz. Path-length induced phase shift would be greater for lower *Q* or a longer path length.

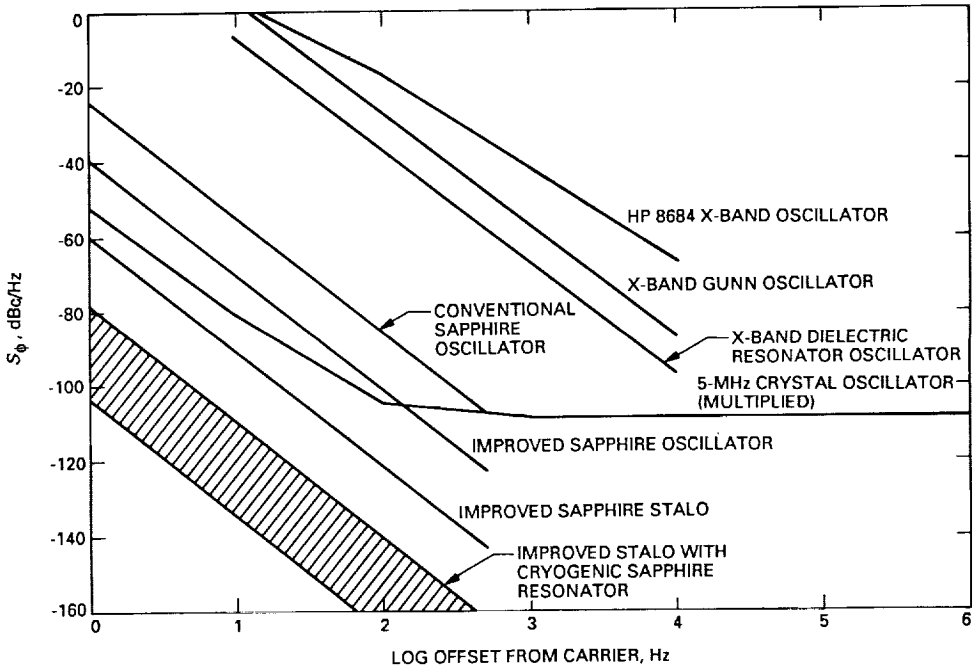

Fig. 12. Phase-noise calculations for improved sapphire whispering-gallery-mode oscillator and STALO shown in Figs. 8 and 7. Use of a cryogenic (170 K to 77 K) sapphire resonator allows further improvement by 20 to 43 dB.